miR-584 and miR-146 are candidate biomarkers for acute respiratory distress syndrome

SIQUAN ZHANG[1*], YINUO HONG[2*], HUAFENG LIU[1], QIANPENG WANG[2], JUAN XU[2], YUJUAN ZHANG[1], XI ZHAO[1], YAN YAO[1], KEXING ZHOU[1] and XIANFENG DING[2]

[1]Intensive Care Unit, XiXi Hospital of Hangzhou, Hangzhou, Zhejiang 310023; [2]College of Life Sciences and Medicine, Zhejiang Sci-Tech University, Hangzhou, Zhejiang 310018, P.R. China

Received May 10, 2020; Accepted October 6, 2020

DOI: 10.3892/etm.2021.9873

Abstract. MicroRNAs (miRNAs/miRs) have important roles in inflammation and infections, which are common manifestations of acute respiratory distress syndrome (ARDS). The present study aimed to assess whether serum miRNAs are potential diagnostic biomarkers for human ARDS. For this, two sets of serum samples from healthy individuals and patients with ARDS were analysed by high-throughput sequencing to identify differentially expressed genes in ARDS. A total of 679 valid sequences were identified as differentially expressed ($P<0.05$). Of these, five differentially expressed miRNAs were subjected to reverse transcription-quantitative PCR validation. Finally, two miRNAs (miR-584 and miR-146a) were successfully verified. These two miRNAs were significantly downregulated in the serum of patients with ARDS. Gene Ontology annotations and Kyoto Encyclopedia of Genes and Genomes pathway analysis revealed that their target transcripts were implicated in a broad range of biological processes and various metabolic pathways, including involvement in the regulation of various inflammatory factors. The present study provided a framework for understanding the molecular mechanisms of ARDS and suggested that miR-584 and miR-146a are associated with ARDS and may be potential therapeutic targets.

Correspondence to: Professor Xianfeng Ding, College of Life Sciences and Medicine, Zhejiang Sci-Tech University, 982 2nd Street, Xiasha Higher Education Park, Jianggan, Hangzhou, Zhejiang 310018, P.R. China
E-mail: xfding@zstu.edu.cn

Ms. Kexing Zhou, Intensive Care Unit, XiXi Hospital of Hangzhou, 2 Hengbu Street, Liuzhen Town, Xihu, Hangzhou, Zhejiang 310023, P.R. China
E-mail: zhouzhoukx@126.com

*Contributed equally

Key words: acute respiratory distress syndrome, high-throughput sequencing, microRNA, Gene Ontology, Kyoto Encyclopedia of Genes and Genomes, signaling pathways

Introduction

Acute respiratory distress syndrome (ARDS) is a severe respiratory disease that results in low oxygen levels in the blood and multiple organ failure (1). Its clinical symptoms include diffuse alveolar injury, oedema, bleeding, the formation of a transparent membrane and polymorphonuclear neutrophil infiltration (2,3). The outcome and risk of ARDS may be influenced by multiple factors and thus, it is difficult to explain the risk and outcome of ARDS with only one clinical factor (4). Furthermore, the characteristics and outcome of ARDS may change over time (5). This means that although individuals are exposed to similar environmental factors, they have different risks of morbidity and survival rates. Depending on these factors, the mortality rate of patients with ARDS is 30-40% (6). It has been speculated that the genome may play an important role in the ARDS (4).

MicroRNAs (miRNAs/miRs) are 21-24 nt duplex RNAs and one miRNA may regulate hundreds of targets (7). Most of the human genome was predicted to be regulated by miRNAs and multiple miRNAs may act cooperatively to silence the same target gene (8). They have important roles in the regulation of post-transcriptional gene expression. Mature miRNAs bind to the 3'-untranslated region of their target gene to control gene expression, resulting in either reduced protein translation or degradation of mRNA (9). With the advances in the current understanding of the genome, miRNAs have been indicated to have an important role in the regulation of numerous biological processes (10). Dysregulation of miRNAs has been identified in various diseases, such as lung cancer (11). In addition, differentially expressed miRNAs are thought to have distinct regulatory roles in biological processes (12). miRNAs, which are non-coding RNA molecules that regulate gene expression at the post-transcriptional level, have emerged as a novel class of gene expression modulators and certain miRNAs have important roles in inflammation and apoptosis, which are common manifestations of ARDS and diffuse alveolar damage (13).

Progress has been made in the study of lung disease on a genome-wide scale and numerous miRNAs have been indicated to be expressed in the lungs (4,14,15). For instance, Yuan *et al* (16) inhibited neutrophilic inflammation by silencing triggering receptor expressed on myeloid cells (TREM-1)

with a nanomicellar approach, suggesting that TREM-1 is a potential therapeutic target for neutrophilic lung inflammation and ARDS. However, studies reporting on the discovery of candidate genes are difficult to replicate due to small sample sizes, population stratification, variability of the control populations or heterogeneity of the ARDS phenotype (4). Thus, the progress of research into biomarkers for ARDS is very slow. However, at the same time, it has been demonstrated that numerous miRNAs are expressed specifically in ARDS compared with normal lung tissue in rat model studies (17,18). For instance, after trauma/transfusion or the physiological remission of ARDS, miR-223 expression increased in the lungs of methyltetradecanoic acid-induced mice or patients with ARDS (19). miR-181a and miR-92a are risk-associated biomarkers for ARDS, whereas miR-424 is a protective biomarker (20). Liu *et al* (21) indicated that upregulation of miRNA-200c-3p reduced the levels of angiotensin-converting enzyme 2, which has a crucial role in the occurrence and development of ARDS.

High-throughput sequencing technology has made it possible to sequence full human genomes and enhance the understanding of genetic effects on diseases, treatment outcomes and public health (22). In the present study, high-throughput sequencing was used to identify differentially expressed miRNAs in the serum of patients with ARDS and reverse transcription-quantitative (RT-q)PCR verification indicated that miR-584 and miR-146a may have important roles in ARDS. miR-122 may have a key role in the progression of ARDS from initiation to death. These genes may be potential targets for the treatment of ARDS.

Materials and methods

Clinical samples. Serum samples of patients with ARDS (age range, 23-85; average age, 63 years; sex ratio, 8:13) and healthy subjects (age range, 27-69; average age, 45 years; sex ratio, 9:11) were collected from December 2013 to February2016, at Xixi Hospital (Hangzhou, China). Healthy samples underwent routine medical examinations at Xixi Hospital. All patients with ARDS met the Berlin diagnostic definition (23): The time of ARDS was within 1 week of a known clinical insult or new or worsening respiratory symptoms; chest imaging indicated bilateral opacities (not fully explained by effusions, lobar/lung collapse or nodules); respiratory failure was not fully explained by cardiac failure or fluid overload; and ARDS severity was based on oxygenation index (arterial oxygen partial pressure/inhaled oxygen concentration). Detailed information on the patients with ARDS is presented in Table I. Serum samples were collected from patients who were grouped according to the two stages of improvement and death. The criteria for selection included an age of ≥18 years; absence of cardiac insufficiency and no pregnancy or lactation. Serum was stored at -80˚C after collection.

RNA extraction and quality control. RNA was extracted by TRIzol reagent (Thermo Fisher Scientific, Inc.) according to the manufacturer's protocol. The NanoDrop-2000 (Thermo Fisher Scientific, Inc.) was used to measure the quantity and quality of RNA. The integrity of RNA was assessed by standard denaturing agarose gel electrophoresis (1%).

High-throughput sequencing. From the 21 cases from the ARDS group and the 20 cases from the healthy group, five serum samples per group were selected. Age, sex, oxygenation index and outcome were evenly distributed among the 5 samples from the ARDS group (Table I). In terms of age, younger (age, 32 years), middle-aged (age, 63 years) and elderly (age, 71, 72 and 81 years) patients were selected. In terms of sex, three females and two males were selected. For the oxygenation index, patients with low (index=58), medium (index=116, 140) and high levels (index=193, 222) were selected. For the final outcome, three patients who died and two patients who finally improved were selected. In terms of clinical diagnosis, patients with H1N1 (n=1) or H7N9 (n=1) infection and patients without special infection were selected. In the healthy group, the age range was 31-69 years and the male-to-female ratio was 3:2. For each group, these 5 samples were mixed for high-throughput sequencing to determine differentially expressed miRNAs. The procedure followed standard Illumina procedures, including library preparation and sequencing. TruSeq Small RNA Sample Prep Kits (Illumina, Inc.) were used to prepare the small RNA sequencing library. After library preparation was completed, Illumina Hiseq2000/2500 (Illumina, Inc.) was used to sequence the constructed library with a single-terminal 1x50-bp reading length.

High-throughput sequencing data analysis. To obtain the clean sequence, ACGT101-miR v4.2 (LC Sciences) was used to remove the 3'adaptor and low-quality sequences. From the remaining sequences, 15 to 27 bp sequences, which were most likely to contain mature miRNAs, were retained for further analysis. miRNA sequences were filtered out and clean data were obtained by comparisons with RFam (http://rfam.janelia.org), Repbase (http://www.girinst.org/repbase) and mRNAbase (ftp://ftp.ensembl.org/pub/release-90/fasta/homo_sapiens/). After comparison with miRNAbase (ftp://mirbase.org/pub/mirbase/CURRENT/), the reads were divided into 4 groups as the follows: 'Group (gp)1'-reads mapped to pre-miRNAs in miRbase and the pre-miRNAs further mapped to the genome and expressed sequence tag; 'gp2'-the mapped pre-miRNAs did not map to the genome, but the reads (and the miRNAs of the pre-miRNAs) mapped to the genome; 'gp3'-reads mapped to selected miRNAs/pre-miRNAs in miRbase, but the mapped pre-miRNAs and the reads did not map to the genome; and 'gp4'-reads did not map to selected pre-miRNAs in miRbase, but the reads mapped to the genome and the extended genome sequences in the genome may form hairpins.

After screening for valid sequences, the expression profiles of these sequences were normalized. Valid sequences were identified in all samples and a reference frame, which consists of the median of the copy number of the relevant valid sequence in all samples, was established. Subsequently, the data of all samples and reference frame data pairs were log2 transformed. The Δlog2 of the log2-transformed data between each respective sample and the reference dataset was calculated and sequences with $|\Delta log2|<2$ were selected. Next, a linear regression analysis of the reference set was performed between samples and subsets to derive the linear formula $y=a_i x+b_i$, where a_i and b_i are the slope and intercept, respectively. For the resulting line, x is the log2 of the reference dataset and

Table I. Information of patients with ARDS.

Patient ID	Age (years)	Sex	Clinical diagnosis	Oxygenation index (mmHg)	Clinical outcome
1[a]	32	Male	Severe measles, severe pneumonia, type I respiratory failure, hepatitis B, hypernatremia.	222	Death
2	47	Male	Measles complicated with pneumonia, respiratory failure, intestinal obstruction.	208	Improvement
3	56	Male	Pulmonary infection, respiratory failure type I, cholestatic hepatitis, parapsoriasis, hypoproteinemia.	161	Improvement
4	58	Male	PCP, pulmonary edema, liver dysfunction.	85	Death
5	66	Male	Chronic renal failure, pulmonary infection, liver cancer after interventional therapy, diabetes mellitus type II, hypertension.	172	Improvement
6	69	Male	Posthepatitic cirrhosis, septic shock, hepatic encephalopathy.	190	Death
7[a]	72	Male	Sepsis, septic shock, severe pulmonary infection, pleural effusion, occupation of left liver space.	116	Improvement
8	83	Male	Cerebral infarction, pulmonary infection, respiratory failure type I, septic shock, senile dementia, myocardial infarction, renal failure.	125	Death
9	23	Female	Severe pneumonia, respiratory failure.	129	Transfer[b]
10	35	Female	Pneumonia, respiratory failure, diabetes mellitus type II.	180	Improvement
11	56	Female	H7N9, severe pneumonia, respiratory failure.	136	Death
12[a]	63	Female	H1N1, pneumonia, post-operative thyroid cancer, diabetes mellitus type II.	193	Improvement
13	69	Female	Respiratory failure type I, severe measles, chronic renal failure.	153	Death
14[a]	71	Female	H7N9, respiratory failure, apoplexy.	140	Death
15	74	Female	Right inguinal hernia, intestinal obstruction, septic shock, cardiac arrest, aspiration pneumonia.	56	Death
16	76	Female	Pulmonary infection, septic shock, respiratory failure, senile emphysema, coronary heart disease.	198	Improvement
17	79	Female	Renal failure, heart failure, pulmonary infection, respiratory failure.	88	Death
19[a]	81	Female	Community-acquired, respiratory failure type I, hypertension, post-operative appendicitis.	58	Death
20	84	Female	Hypertension, respiratory failure, sepsis, septic shock, severe pulmonary infection.	76	Transfer[b]
21	85	Female	Pulmonary edema, stroke, liver cirrhosis, respiratory failure.	103	Transfer[b]

[a]Samples selected for sequencing. [b]Patient was transferred to a different hospital according to their families' wishes. All patients were treated with pressure control ventilation.

y is the expected value log2 of sample i on a corresponding sequence. The median value of the reference frame, xmid, was then calculated as xmid=[max(x)-min(x)]/2. The log2 of the relevant sample i was calculated as $y_{i,\ mid}=a_i x_{mid} + b_i$, such that $y_{r,\ mid}=x_{mid}$ and $\Delta y_i=y_{r,\ mid}-y_{i,\ mid}$, which is the logarithmic correction factor of sample i. The correction factor algorithm for sample i $f_i=2^{\Delta yi}$ was then obtained. The number of copies for each sample was obtained by multiplying the original copy number with the algorithm correction factor f_i.

RT-qPCR. Candidate miRNA selection was based on the following criterion: Fold-change >2 after data normalization. Patients were divided into the disease group (n=8) and the death group (n=10) according to whether the final clinical symptoms were improved or the patient died, and three patients were transferred to a different hospital according to their families' wishes, so they were not included in the disease group or death group. A total of five randomly selected miRNAs were validated by RT-qPCR. The stem-loop

Table II. Stem-loop primers used for reverse-transcription PCR.

Name	Sequence (5'-3')
miR-584	GTCGTATCCAGTGCGTGTCGTGGAGTCGGCAATTGCACTGGATACGACCTCAGTC
miR-451	GTCGTATCCAGTGCGTGTCGTGGAGTCGGCAATTGCACTGGATACGACAACTCAG
miR-146a	GTCGTATCCAGTGCGTGTCGTGGAGTCGGCAATTGCACTGGATACGACAACCCAT
miR-193a	GTCGTATCCAGTGCGTGTCGTGGAGTCGGCAATTGCACTGGATACGACTCATCTC
miR-122	GTCGTATCCAGTGCGTGTCGTGGAGTCGGCAATTGCACTGGATACGACCAAACAC

miR, microRNA.

Table III. Sequences of primers used for quantitative PCR.

Name	Forward primer (5'-3')	Reverse primer[a] (5'-3')
hsa-miR-584	GGTTATGGTTTGCCTGGGA	
hsa-miR-451	CCCCAAACCGTTACCATTACT	
hsa-miR-146a	GGGGTGAGAACTGAATTCCAT	CAGTGCGTGTCGTGGAGT
hsa-miR-193a	GGGTCTTTGCGGGCG	
hsa-miR-122	GGTGGAGTGTGACAATGGTG	
5S rRNA	GTCTACGGCCATACCACCCTGAA	AAGCCTACAGCACCCGGTATTCC

[a]The reverse primer is a universal reverse primer. miR, microRNA; hsa, *Homo sapiens*.

primers used for RT of miRNAs (http://primer3.ut.ee/) are listed in Table II. Complementary DNA was synthesized using M-MLV(H-) Reverse Transcriptase obtained from Vazyme Biotechnology. M-MLV(H-) Reverse Transcriptase (Vazyme Biotech), 5x RT Buffer (Vazyme Biotech), dNTP Mixture (Vazyme Biotech), primer (Sangon Biotech), RNase Inhibitor (Vazyme Biotech) and ddH_2O are included in the reverse transcription reaction system. The temperature protocol for reverse transcription was as follows: 45 min at 42˚C, 5 min at 85˚C. The reaction was carried out in a PCR instrument (cat. no. T1000; Bio-Rad Laboratories, Inc.). qPCR was performed with SYBR Green qPCR (Toyobo) according to the manufacturer's protocol. The composition of this reaction mixture included the primers (Sangon Biotech), SYBR Green qPCR Mix (Toyobo) and ddH_2O. The temperature protocol for reverse transcription was as follows: Initial denaturation 95˚C for 30 sec, followed by 40 cycles of 95˚C for 10 sec and 60˚C for 30 sec. The reaction was carried out in a qPCR instrument (7500; Applied Biosystems; Thermo Fisher Scientific, Inc.). 5S ribosomal RNA was used as an internal control. Relative mRNA expression of each gene compared to 5S ribosomal RNA was calculated using the $2^{-\Delta\Delta Cq}$ method (24). The primer information of miRNAs for qPCR is provided in Table III. All miRNAs had the same stem-loop sequence. The reverse primer used for qPCR was designed based on the stem-loop sequence and thus, it was a universal reverse primer.

miRNA and mRNA co-expression network. Based on the results of the sequence analysis, the following five miRNAs with the largest difference in expression levels were obtained: miR-584, miR-451, miR-146a, miR-193a and miR-122. miRDB (http://mirdb.org), miRWalk (http://mirwalk.umm.uni-heidelberg.de) and TargetScan 7.0 (http://www.targetscan.org/vert_72/) were used for target gene prediction.

Gene Ontology (GO) enrichment and Kyoto Encyclopedia of Genes and Genomes (KEGG) analysis. GO annotations of target genes corresponding to differentially expressed miRNAs were performed with the WEB-based GEne SeT AnaLysis Toolkit (http://www.webgestalt.org/option.php). KEGG pathways were analysed through KEGG Mapper (https://www.kegg.jp/kegg/mapper.html) to identify the significant pathways of the differentially expressed genes. GO terms and KEGG pathways with a corrected P-value <0.05, which was calculated by the hypergeometric test, were considered to be significantly enriched. Futhermore, -log10(P) was used to determine the enrichment of each GO term by the differentially expressed genes and the significance of the pathway associations.

Statistical analysis. All statistical analyses were conducted with SPSS (20.0 IBM Corp.). Statistical comparisons of the sequencing data were performed using Student's t-test. ANOVA was used for comparisons between multiple groups, followed by the Least-Significant Difference test. P<0.05 was considered to indicate a statistically significant difference.

Results

Processing of raw miRNA high-throughput sequencing data. A total of $1.8x10^7$ raw-sequence reads from the serum of patients with ARDS and $1.9x10^7$ raw-sequence reads from the serum of healthy subjects were obtained. In the filtering

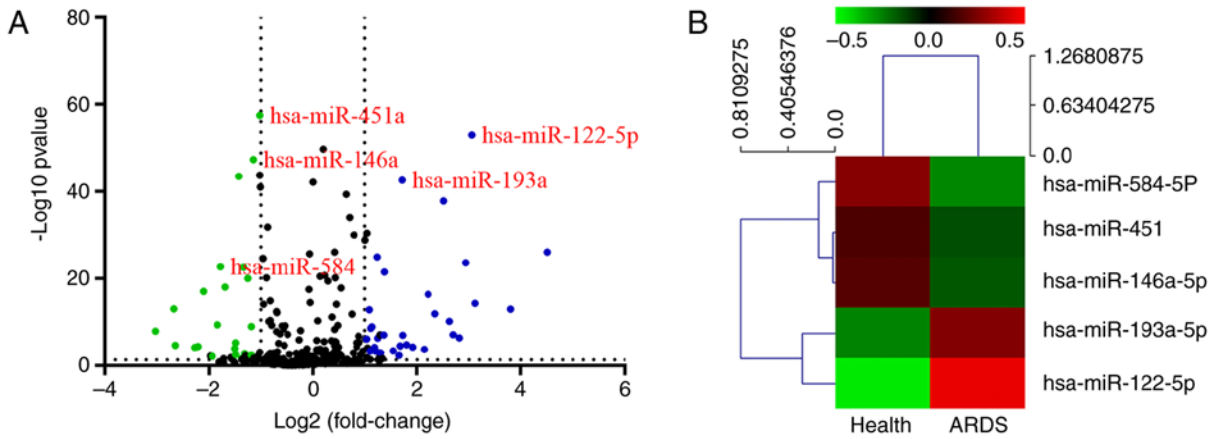

Figure 1. Analysis of differentially expressed miRNAs. (A) Volcano plot indicating the differentially expressed miRNAs. Blue dots represent significantly upregulated miRNAs, green dots represent significantly downregulated miRNAs and black points represent miRNAs that were not significantly different between the ARDS and healthy groups. The two vertical lines indicate the filtering standard of fold-change ≥2. (B) Clustering analysis of differences in serum levels of miRNAs between the ARDS and healthy groups. In the heat map, the highly upregulated genes are indicated in red the downregulated genes are displayed in green. Because the samples for each group were pooled, there is only one entry for each group. miRNA/miR, microRNA; ARDS, acute respiratory distress syndrome; hsa, *Homo sapiens*.

analysis, a total of 679 miRNAs were identified to be differentially expressed between the ARDS and healthy samples. Of the 679 miRNAs, 537 miRNAs belonged to the category gp1, 17 miRNAs to gp2, 24 miRNAs to gp3 and 101 miRNAs to gp4. In gp1 and gp2, 112 miRNAs were selected according to the screening conditions fold-change >2 and P<0.05. A total of 55 miRNAs were upregulated, while 57 miRNAs were downregulated. In the volcano plot analysis of the differentially expressed miRNAs, the ARDS group was successfully separated from the normal group (Fig. 1A). The top 5 differentially expressed miRNAs are presented in a heat map in Fig. 1B. miR-584, miR-451, miR-146a and miR-193a were the most downregulated miRNAs, while miR-122 was the most upregulated.

Validation of differentially expressed miRNAs in ARDS and healthy serum by RT-qPCR. To confirm the previous results and identify the functions of miRNAs in ARDS, five randomly selected miRNAs (Table IV), including three downregulated miRNAs, *Homo sapiens* (hsa)-miR-584, hsa-miR-451 and hsa-miR-146a, and two upregulated miRNAs, hsa-miR-193a and hsa-miR-122, were validated by RT-qPCR (Fig. 2).

The results were similar to those of the high-throughput sequencing. High-throughput sequencing and RT-qPCR demonstrated downregulated expression of hsa-miR-584 and hsa-miR-146a and upregulated expression of hsa-miR-122 in the disease vs. healthy group (Fig. 2A). However, in the death vs. healthy group, miR-122 was downregulated (Fig. 2B). In the comparison of the death vs. healthy group, only the results of hsa-miR-584 and hsa-miR-146a were similar to those of the high-throughput sequencing (Fig. 2C). To reduce the individual differences for sequencing, the samples were pooled in the sequencing analysis, mixing patients from the disease and death groups; thus, the sequencing results did not reflect the differences between the disease group and the death group.

Prediction of potential miRNA targets. As miRNAs affect gene expression by regulating mRNAs, the target mRNAs of the miRNAs were predicted in a further analysis. miR-584 and miR-146a were selected for target gene prediction due to their significant differences. ViennaRNA Web Services (http://nibiru.tbi.univie.ac.at/forna/) were used to plot the secondary structures of the miR-584 and miR-146 precursors (Fig. 3A and B). MiRDB, miRWalk and TargetScan 7.0 were used for this prediction and the results were intersected. A total of 134 target genes were predicted for miR-584 and 41 target genes for miR-146a (Fig. 3C and D). Analysis of the network map of the target genes of these two miRNAs identified only two common target genes (Fig. 3E).

GO analysis. GO enrichment analysis of significantly differentially expressed mRNAs was performed to determine the effects of these miRNAs. The WEB-based GEne SeT AnaLysis Toolkit (webgestalt; http://www.webgestalt.org/option.php) was used to annotate the potential biological functions and signalling pathways of the target genes. GO categories of 'biological process' (BP), 'cellular component' (CC) and 'molecular function' (MF) were analysed to determine gene functions and gene product enrichment. The results of the GO enrichment analysis are presented in Fig. 4. The analysis revealed that the majority of the BP terms associated with both miR-146a (Fig. 4A) and miR-584 (Fig. 4B) were involved in the processes of cell life activity and composition, such as 'biological regulation', 'metabolic process', 'multicellular organismal process' and 'cellular component organization'. In the category CC, the terms of the target mRNAs of miR-146a and miR-584 included 'nucleus', 'membrane' and 'macromolecular complex'. In the MF category, the target mRNAs were enriched in terms associated with binding activities, including 'protein binding', 'ion binding' and 'nucleic acid binding'.

KEGG analysis. The results of the KEGG pathway enrichment analysis of target mRNAs are presented in Fig. 5 and pathways with P<0.05 were selected to draw a bubble diagram. These results demonstrated that the target mRNAs of hsa-miRNA-584 may be involved in 'ubiquitin-mediated

Table IV. Details of the 5 randomly selected miRNAs for reverse transcription-quantitative PCR confirmation.

miRNA name	P-value	Fold-change	Direction of regulation	Chromosome	Strand	Expression
hsa-miR-584	$1.93x10^{-23}$	0.29	Down	Chr5	-	Middle
hsa-miR-451a	$3.36x10^{-44}$	0.49	Down	Chr17	-	High
hsa-miR-146a	$4.86x10^{-83}$	0.45	Down	Chr5	+	High
hsa-miR-193a	$2.85x10^{-110}$	3.29	Up	Chr17	+	Middle
hsa-miR-122	$2.94x10^{-26}$	8.32	Up	Chr18	+	High

miR/miRNA, microRNA; hsa, *Homo sapiens*; Chr, chromosome; + strand, sense strand; - strand, antisense strand.

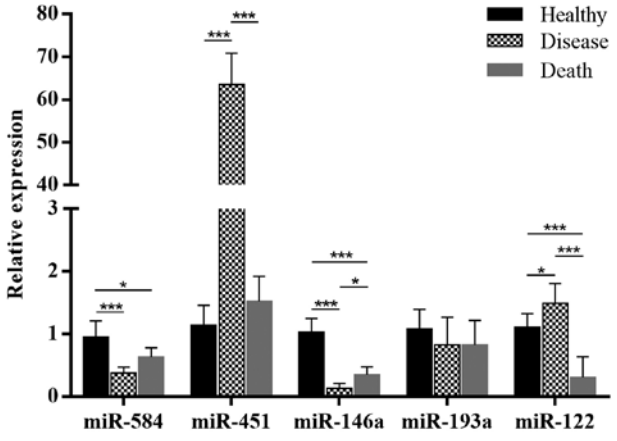

Figure 2. Validation of the microarray data by reverse transcription-quantitative PCR. miRNA expression levels in the healthy (n=20), disease (n=8) group and death (n=10) groups. ANOVA was used for comparative analysis, followed by a Least-Significant Difference test. *P<0.05 and ***P<0.001. miRNA/miR, microRNA.

proteolysis', 'sulfur metabolism', 'retrograde endocannabinoid signaling' and 'regulation of actin cytoskeleton' (Fig. 5A). In addition, 'tuberculosis', 'toxoplasmosis', 'Toll-like receptor (TLR) signaling pathway' and 'NF-κB signaling pathway' were associated with the target mRNAs of hsa-miR-146a (Fig. 5B). MAPK cascade activation is the hub of multiple signalling pathways and NF-κB is one of the downstream effectors of the MAPK signalling pathway (25). Thus, further analysis focused on the MAPK signaling pathway. According to the KEGG prediction, glial cell line-derived neurotrophic factor (GDNF), which is a target gene of miR-146a, and RAB23, which belongs to the RAS family and is a target gene of miR-584, are involved in the MAPK signalling pathway, which is an inflammation-associated signalling pathway (26) (Fig. 5C).

Discussion

At present, no sensitive or specific biomarker for the early diagnosis and treatment of ARDS is available. Considering the high risk of death with ARDS, particularly in children (27), further investigations into the molecular mechanisms of ARDS are crucial to improve the survival rate. ARDS is a multifactorial syndrome with high morbidity and mortality rates, despite an enhanced understanding of ARDS pathogenesis, the capacity to predict the development of ARDS remains limited (28). miRNAs have emerged as critical molecules in human diseases (13,29-31). However, a limited number of studies on miRNAs associated with the pathogenesis and progression of ARDS have been published.

In the present study, using high-throughput sequencing technology, a preliminary molecular analysis of miRNAs and mRNAs in ARDS was performed to facilitate further studies on the pathogenesis of ARDS and to explore whether the pathology of ARDS may be induced by novel miRNAs. In addition, GO and KEGG pathway enrichment analyses were performed to identify the potential functions of differentially expressed mRNAs.

Comparison of the expression profiles of miRNAs in ARDS and healthy samples provided 679 differentially expressed miRNAs. The most upregulated or downregulated miRNAs may help identify molecular markers for the early diagnosis of ARDS. A total of five miRNAs were randomly selected for RT-qPCR validation and the results of only 3 miRNAs were consistent with the sequencing analysis. This may be because a pooled sample strategy was adopted during sequencing, while in the RT-qPCR analysis, a more detailed grouping was performed. After excluding the difference between the disease group and the death group, the sequencing results were still reliable.

GO enrichment analysis was used to identify the functions of the miRNAs through the expression patterns of their target mRNAs. Among the target mRNAs of miR-146a and miR-584, most of the BP terms were associated with cell activity and composition. Alveolar macrophages and alveolar epithelial cells are the first line of host defence and innate immunity (32). In addition to macrophages and alveolar epithelial cells, leukocytes and endothelial cells are also essential for the inflammatory response in acute lung injury (ALI)/ARDS. In addition, regulating the function of macrophages and monocytes may be a promising therapeutic strategy against ALI/ARDS (33). This evidence may indicate that the differentially expressed miRNAs are associated with the activities and functions of these immune cells.

The enriched CC terms were associated with the nucleus and membrane, which are key organelles for biological regulation, protein formation and secretion. As discussed above, macrophages are important in ARDS, both in terms of pro-inflammatory and anti-inflammatory activities (34). In addition, NF-κB is a key transcription factor in the regulation of the innate immune inflammatory response in activated macrophages (35). Activation of the NF-κB signalling pathway

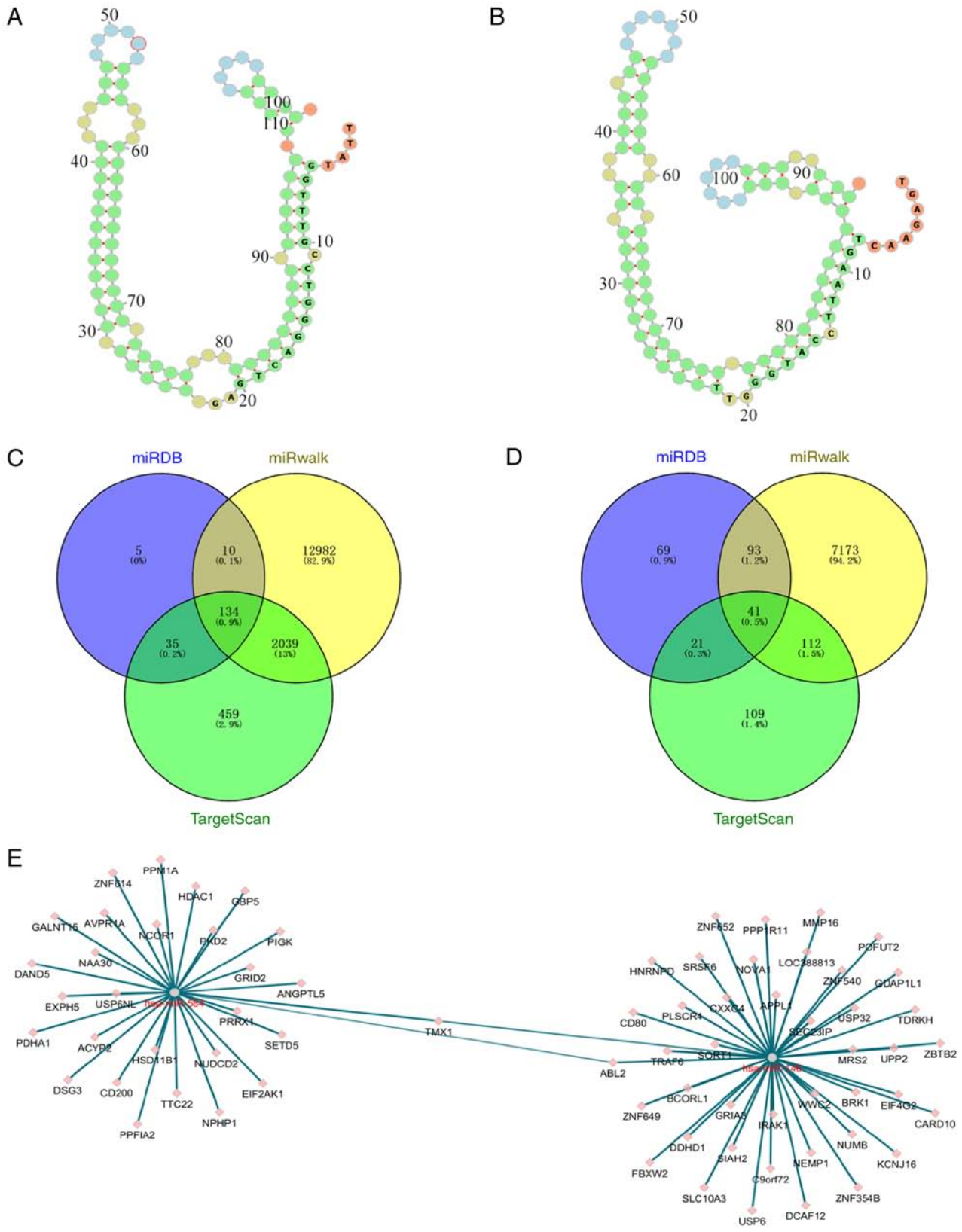

Figure 3. Two-dimensional structure analysis and target gene prediction of miR-584 and miR-146a. Based on the sequencing results, the secondary structure of (A) miR-584 and (B) miR-146a precursors was predicted. Venn diagrams indicating the number of common and target genes for (C) miR-584 and (D) miR-146a in the three databases miRDB, miRwalk and TargetScan. (E) Comparison between the target genes of miR-584 and miR-146 revealed that there were two identical target genes. miR, microRNA; hsa, *Homo sapiens*.

requires extracellular factors to stimulate receptors on the cell membrane and free NF-κB is required to enter the nucleus to initiate transcription (36). Members of the IL-1 family are key determinants of inflammation. They mainly participate in the inflammatory response through membrane processes, including direct plasma membrane translocation, lysosome

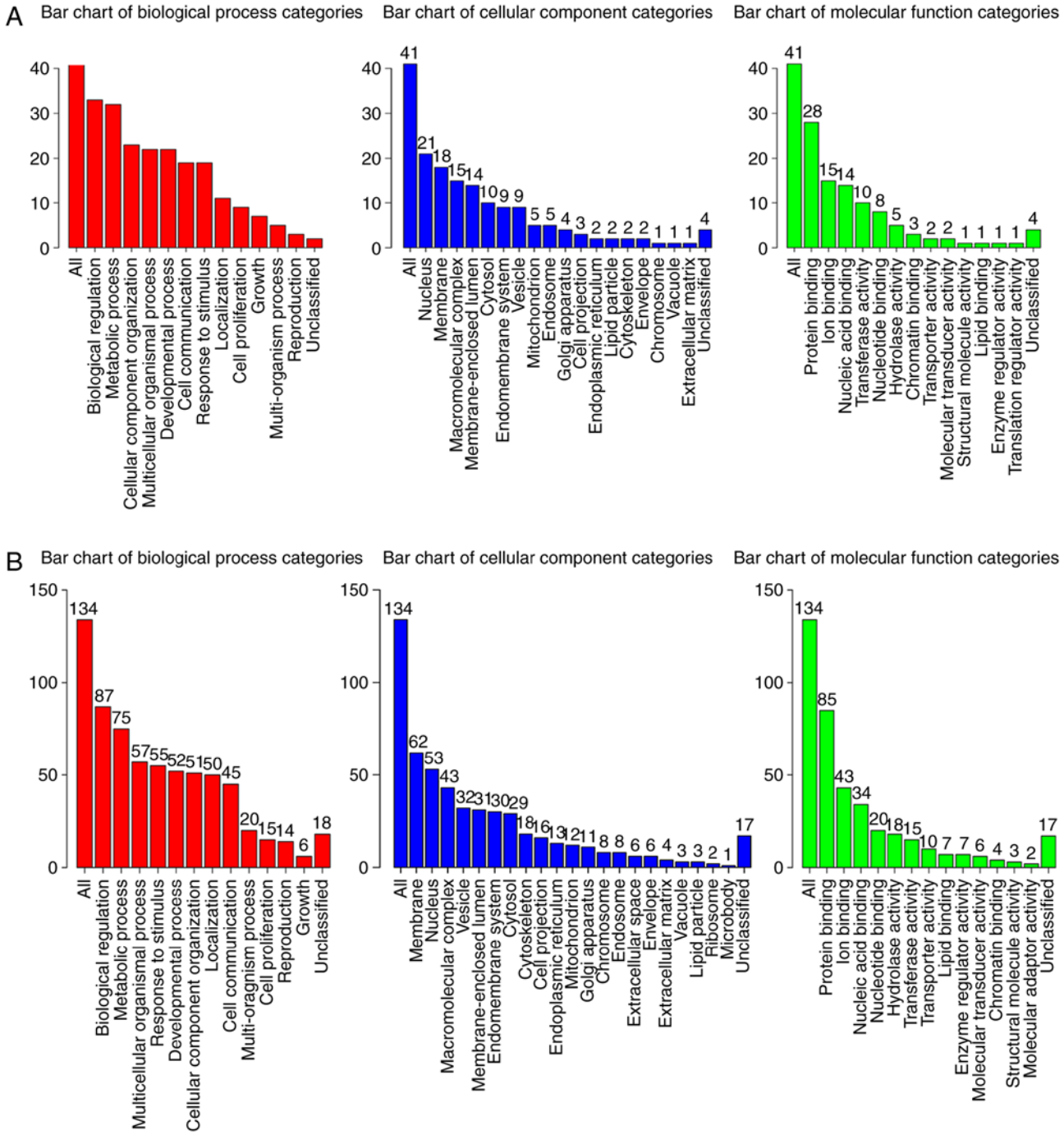

Figure 4. Gene Ontology analysis of the predicted target genes of (A) miR-146a and (B) miR-584 in the categories Biological Process, Cellular Component and Molecular Function. The number of genes accumulated in each term is displayed on the Y-axis. miR, microRNA.

exocytosis, exosome formation, membrane vesiculation, autophagy and pyroptosis (37).

The MF terms were associated with protein binding and ion binding. After the NF-κB signalling pathway is activated, NF-κB binds to multiple proteins or factors to mediate its effector functions (38). In addition, numerous studies have indicated that zinc modulates the NF-κB pathway (39). This is consistent with the results of the GO enrichment analysis in the present study.

KEGG pathway enrichment analysis revealed that pathways such as 'ubiquitin-mediated proteolysis', 'sulfur metabolism' and 'regulation of actin cytoskeleton' were associated with the target mRNAs of miR-584. NF-κB is a critical transcription factor for the maximal expression of numerous cytokines that are involved in the pathogenesis of inflammatory diseases, such as ARDS and sepsis syndrome. NF-κB activation involves the phosphorylation, ubiquitination and proteolysis of IκB (40). There is also experimental evidence that the actin cytoskeleton has an important role in the regulation of NF-κB activation and inflammatory events in intestinal epithelial cells (41). Numerous studies have proven that sulphides directly or indirectly affect the NF-κB signalling pathway, but they focused on a specific sulphide, not the entire sulfur metabolism system (42-44). The enrichment analysis of miR-584 target genes is basically consistent with previous experiments.

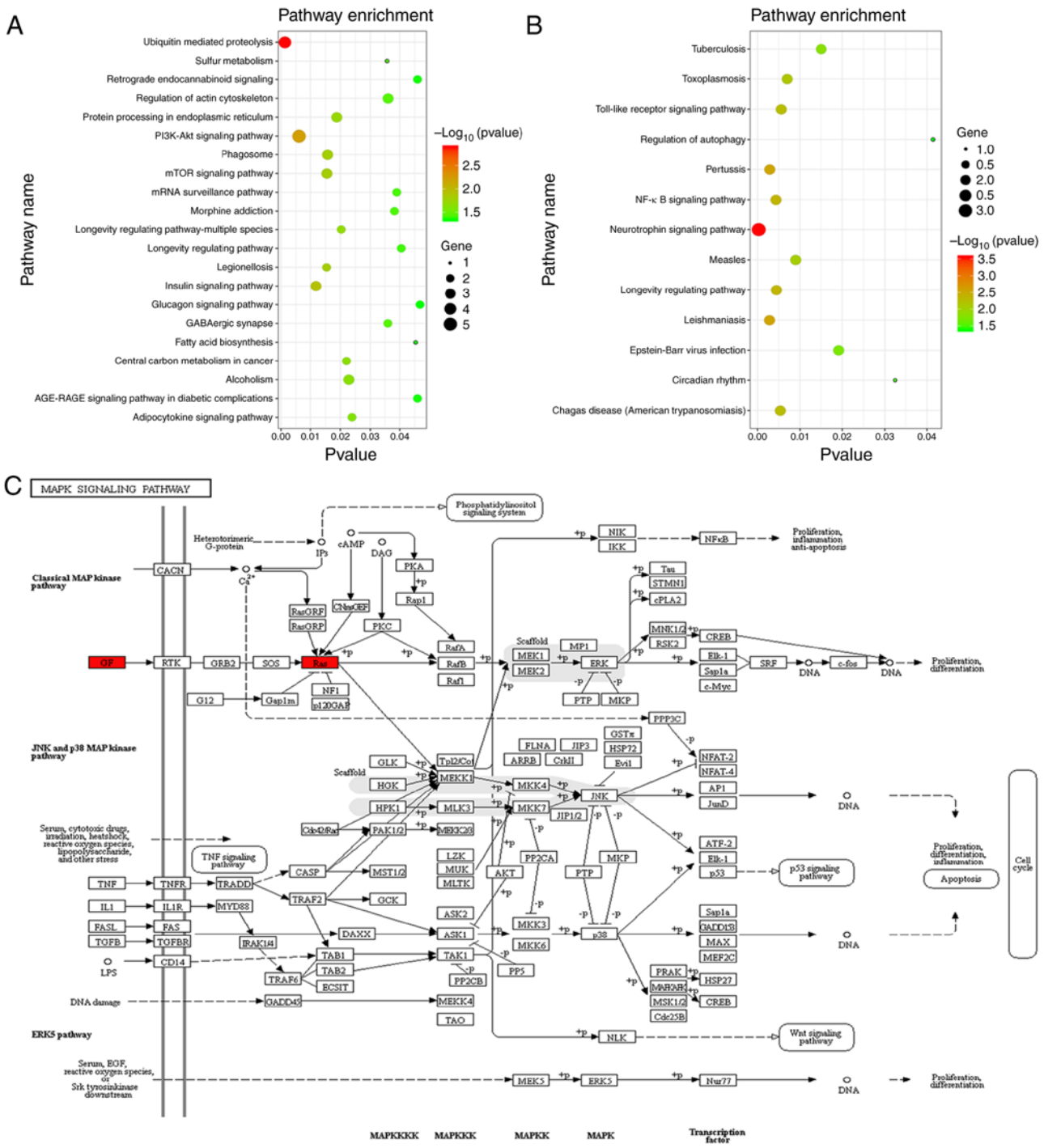

Figure 5. Bubble chart of the Kyoto Encyclopedia of Genes and Genomes pathway enrichment analysis (P<0.05) for (A) miR-146a and (B) miR-584. The richfactor (the value of the P-value divided by the q-value, and q-value is the adjusted P-value) is displayed on the X-axis of the bubble chart. The size of the bubbles represents the number of genes involved. The colour of the bubbles represents-log10 (P-value). (C) Gene/pathway interaction map. The target gene of miR-146a, GDNF, belongs to the GF family and the target gene of miR-584, RAB23, belongs to the Ras family; both of them participate in the MAPK signaling pathway. miR, microRNA.

Pathways such as 'tuberculosis', 'toxoplasmosis', 'TLR signaling pathway' and 'NF-κB signaling pathway' were associated with the target mRNAs of miR-146a. The TLR family acts as a primary sensor of innate immunity and all TLR signalling pathways culminate with the activation of the transcription factor NF-κB (45). Numerous studies have proven that miR-146a is closely related to inflammation (46-48). There is also considerable evidence that miR-146a is closely linked to lung diseases, including ARDS (49-51). The results of the target gene enrichment in the present study are consistent with previous results.

One of the predicted target genes of miR-146a, GDNF, is involved in the development of pulmonary innervation (52). Certain studies have proven that the introduction of the GDNF gene into macrophages may effectively reduce neuronal inflammation (53). RAB23 is a predicted target gene of miR-584. Huang *et al* (54) detected the expression of Rab23

protein in the nuclei in lung cancer tissues by immunohistochemistry. Furthermore, the dysregulation of RAB23 may affect the NF-κB signalling pathway (55). The predictions of the present study are consistent with these findings.

A limitation of the present study is the focus on high-throughput analysis and the related miRNA-mRNA network, GO analysis and KEGG analysis based on the predicted targeted genes. Further research on miRNA functions will be performed in future studies with the aim of obtaining additional evidence to corroborate the bioinformatics predictions.

In conclusion, the results of the present study suggested that miRNA-584 and miR-146a may be involved in the occurrence and development of inflammation in ARDS by affecting macrophages, and NF-κB may have an important role in this process. These molecules may be promising therapeutic targets for patients with ARDS and further studies are required to explore the precise mechanisms of ARDS.

Overall, it was revealed that miR-584, miR-146a and miR-122 have a certain association with ARDS and may be potential therapeutic targets. However, certain limitations of the present study should also be acknowledged. Of note, the results were only based on 21 serum samples from patients with ARDS. There may be certain false-positives and further verification is required. Future research on these targets is required to validate the functions of the identified miRNAs in ARDS and provide a more comprehensive understanding of the underlying mechanisms.

Acknowledgements

Not applicable.

Funding

This work was supported by grants from the Department of Health of Zhejiang Province (grant no. 2019322603) and the Hangzhou Science and Technology Bureau (grant no. 20191223B75).

Availability of data and materials

All data generated or analysed during this study are included in this published article.

Authors' contributions

SZ and YH made substantial contributions to the conception or design of the study and drafting the manuscript or revising it critically for important intellectual content. HL, JX, QW, YZ, XZ and YY collected, analysed or interpreted data. XD edited and critically revised the manuscript. KZ proposed the experimental idea and participated in the design of the experiment. XD is the main designer of the experiment specifically performing the experiments, and data collection. KZ ensured that questions relating to the accuracy or completeness of any part of the work are properly investigated and resolved. All authors read and approved the final version of the manuscript.

Ethics approval and consent to participate

The study protocol was approved by the Human Ethics Review Committee at XiXi Hospital of Hangzhou and Zhejiang Sci-Tech University (Hangzhou, China). All participants provided written informed consent prior to enrolment.

Patient consent for publication

Not applicable.

Competing interests

The authors declare that they have no competing interests.

References

1. Holland MC, Mackersie RC, Morabito D, Campbell AR, Kivett VA, Patel R, Erickson VR and Pittet JF: The development of acute lung injury is associated with worse neurologic outcome in patients with severe traumatic brain injury. J Trauma 55: 106-111, 2003.
2. Katzenstein AL, Bloor CM and Leibow AA: Diffuse alveolar damage- the role of oxygen, shock, and related factors. Am J Pathol 85: 209-228, 1976.
3. Ware LB and Matthay MA: The acute respiratory distress syndrome. N Engl J Med 342: 1334-1349, 2000.
4. Reilly JP, Christie JD and Meyer NJ: Fifty years of research in ARDS. Genomic contributions and opportunities. Am J Respir Crit Care Med 196: 1113-1121, 2017.
5. Ferring M and Vincent JL: Is outcome from ARDS related to the severity of respiratory failure? Eur Respir J 10: 1297-1300, 1997.
6. Rubenfeld GD, Caldwell E, Peabody E, Weaver J, Martin DP, Neff M, Stern EJ and Hudson LD: Incidence and outcomes of acute lung injury. N Engl J Med 8: 1685-1693, 2005.
7. Wang Y, Brahmakshatriya V, Zhu H, Lupiani B, Reddy SM, Yoon BJ, Gunaratne PH, Kim JH, Chen R, Wang J and Zhou H: Identification of differentially expressed miRNAs in chicken lung and trachea with avian influenza virus infection by a deep sequencing approach. BMC Genomics 10: 512, 2009.
8. Lu J and Clark AG: Impact of microRNA regulation on variation in human gene expression. Genome Res 22: 1243-1254, 2012.
9. Lu Y, Okubo T, Rawlins E and Hogan BL: Epithelial progenitor cells of the embryonic lung and the role of microRNAs in their proliferation. Proc Am Thorac Soc 5: 300-304, 2008.
10. Bartel DP: MicroRNAs: Genomics, biogenesis, mechanism, and function. Cell 116: 281-297, 2004.
11. Croce CM: Causes and consequences of microRNA dysregulation in cancer. Nat Rev Genet 10: 704-714, 2009.
12. Li J, Aung LH, Long B, Qin D, An S and Li P: miR-23a binds to p53 and enhances its association with miR-128 promoter. Sci Rep 5: 16422, 2015.
13. Ferruelo A, Penuelas O and Lorente JA: MicroRNAs as biomarkers of acute lung injury. Ann Transl Med 6: 34-44, 2018.
14. Orwoll BE and Sapru A: Biomarkers in pediatric ARDS: Future directions. Front Pediatr 4: 55, 2016.
15. Rajasekaran S, Pattarayan D, Rajaguru P, Sudhakar Gandhi PS and Thimmulappa RK: MicroRNA regulation of acute lung injury and acute respiratory distress syndrome. J Cell Physiol 231: 2097-2106, 2016.
16. Yuan Z, Syed M, Panchal D, Joo M, Bedi C, Lim S, Onyuksel H, Rubinstein I, Colonna M and Sadikot RT: TREM-1-accentuated lung injury via miR-155 is inhibited by LP17 nanomedicine. Am J Physiol Lung Cell Mol Physiol 310: L426-L438, 2016.
17. Huang C, Xiao X, Chintagari NR, Breshears M, Wang Y and Liu L: MicroRNA and mRNA expression profiling in rat acute respiratory distress syndrome. BMC Med Genomics 7: 46, 2014.
18. Guan Y, Jin X, Liu X, Huang Y, Wang M and Li X: Identification of microRNAs in acute respiratory distress syndrome based on microRNA expression profile in rats. Mol Med Rep 16: 3357-3362, 2017.

19. Feng Z, Qi S, Zhang Y, Qi Z, Yan L, Zhou J, He F, Li Q, Yang Y, Chen Q, *et al*: Ly6G+ neutrophil-derived miR-223 inhibits the NLRP3 inflammasome in mitochondrial DAMP-induced acute lung injury. Cell Death Dis 8: e3170, 2017.
20. Zhu Z, Liang L, Zhang R, Wei Y, Su L, Tejera P, Guo Y, Wang Z, Lu Q, Baccarelli AA, *et al*: Whole blood microRNA markers are associated with acute respiratory distress syndrome. Intensive Care Med Exp 5: 38, 2017.
21. Liu Q, Du J, Yu X, Xu J, Huang F, Li X, Zhang C, Li X, Chang J, Shang D, *et al*: miRNA-200c-3p is crucial in acute respiratory distress syndrome. Cell Discov 3: 17021, 2017.
22. Goldfeder RL, Wall DP, Khoury MJ, Ioannidis JPA and Ashley EA: Human genome sequencing at the population scale: A primer on High-throughput DNA sequencing and analysis. Am J Epidemiol 186: 1000-1009, 2017.
23. de Luis Cabezón N, Sánchez Castro I, Bengoetxea Uriarte UX, Rodrigo Casanova MP, García Peña JM and Aguilera Celorrio L: Acute respiratory distress syndrome: A review of the Berlin definition. Rev Esp Anestesiol Reanim 61: 319-327, 2014 (In Spanish).
24. Livak KJ and Schmittgen TD: Analysis of relative gene expression data using real-time quantitative PCR and the 2(-Delta Delta C(T)) method. Methods 25: 402-408, 2001.
25. Seger R and Krebs EG: The MAPK signaling cascade. FASEB J 9: 726-735, 1995.
26. Kaminska B: MAPK signalling pathways as molecular targets for anti-inflammatory therapy-from molecular mechanisms to therapeutic benefits. Biochim Biophys Acta 1754: 253-262, 2005.
27. Monahan LJ: Acute respiratory distress syndrome. Curr Probl Pediatr Adolesc Health Care 43: 278-284, 2013.
28. Capelozzi VL, Allen TC, Beasley MB, Cagle PT, Guinee D, Hariri LP, Husain AN, Jain D, Lantuejoul S, Larsen BT, *et al*: Molecular and immune biomarkers in acute respiratory distress syndrome: A perspective from members of the pulmonary pathology society. Arch Pathol Lab Med 141: 1719-1727, 2017.
29. Bekris LM and Leverenz JB: The biomarker and therapeutic potential of miRNA in Alzheimer's disease. Neurodegener Dis Manag 5: 61-74, 2015.
30. Qadir MI and Faheem A: miRNA: A diagnostic and therapeutic tool for pancreatic cancer. Crit Rev Eukaryot Gene Expr 27: 197-204, 2017.
31. Rupaimoole R and Slack FJ: MicroRNA therapeutics: Towards a new era for the management of cancer and other diseases. Nat Rev Drug Discov 16: 203-222, 2017.
32. Lee H, Abston E, Zhang D, Rai A and Jin Y: Extracellular vesicle: An emerging mediator of intercellular crosstalk in lung inflammation and injury. Front Immunol 9: 924, 2018.
33. Huang X, Xiu H, Zhang S and Zhang G: The Role of Macrophages in the Pathogenesis of ALI/ARDS. Mediators Inflamm 2018: 1264913, 2018.
34. Ye C, Li H, Bao M, Zhuo R, Jiang G and Wang W: Alveolar macrophage-derived exosomes modulate severity and outcome of acute lung injury. Aging (Albany NY) 12: 6120-6128, 2020.
35. Ernst O, Vayttaden SJ and Fraser IDC: Measurement of NF-κB activation in TLR-activated macrophages. Methods Mol Biol 1714: 67-78, 2018.
36. Napetschnig J and Wu H: Molecular basis of NF-κB signaling. Annu Rev Biophys 42: 443-468, 2013.
37. Sitia R and Rubartelli A: Evolution, role in inflammation, and redox control of leaderless secretory proteins. J Biol Chem 295: 7799-7811, 2020.
38. Hoesel B and Schmid JA: The complexity of NF-κB signaling in inflammation and cancer. Mol Cancer 12: 86, 2013.
39. Jarosz M, Olbert M, Wyszogrodzka G, Młyniec K and Librowski T: Antioxidant and anti-inflammatory effects of zinc. Zinc-dependent NF-κB signaling. Inflammopharmacology 25: 11-24, 2017.
40. Blackwell TS and Christman JW: The role of nuclear factor-kappa B in cytokine gene regulation. Am J Respir Cell Mol Biol 17: 3-9, 1997.
41. Németh ZH, Deitch EA, Davidson MT, Szabó C, Vizi ES and Haskó G: Disruption of the actin cytoskeleton results in nuclear factor-kappaB activation and inflammatory mediator production in cultured human intestinal epithelial cells. J Cell Physiol 200: 71-81, 2004.
42. Chi Q, Wang D, Hu X, Li S and Li S: Hydrogen sulfide gas exposure induces necroptosis and promotes inflammation through the MAPK/NF-κB Pathway in Broiler Spleen. Oxid Med Cell Longev 2019: 8061823, 2019.
43. Benedetti F, Davinelli S, Krishnan S, Gallo RC, Scapagnini G, Zella D and Curreli S: Sulfur compounds block MCP-1 production by Mycoplasma fermentans-infected macrophages through NF-κB inhibition. J Transl Med 12: 145, 2014.
44. Ruff AL and Dillman JF III: Sulfur mustard induced cytokine production and cell death: Investigating the potential roles of the p38, p53, and NF-kappaB signaling pathways with RNA interference. J Biochem Mol Toxicol 24: 155-164, 2010.
45. Kawai T and Akira S: Signaling to NF-kappaB by Toll-like receptors. Trends Mol Med 13: 460-469, 2007.
46. Pfeiffer D, Roßmanith E, Lang I and Falkenhagen D: miR-146a, miR-146b, and miR-155 increase expression of IL-6 and IL-8 and support HSP10 in an In vitro sepsis model. PLoS One 12: e0179850, 2017.
47. Li Y, Zhu H, Wei X, Li H, Yu Z, Zhang H and Liu W: LPS induces HUVEC angiogenesis in vitro through miR-146a-mediated TGF-β1 inhibition. Am J Transl Res 9: 591-600, 2017.
48. Du L, Chen X, Duan Z, Liu C, Zeng R, Chen Q and Li M: miR-146a negatively regulates dectin-1-induced inflammatory responses. Oncotarget 8: 37355-37366, 2017.
49. Shi L, Xu Z, Wu G, Chen X, Huang Y, Wang Y, Jiang W and Ke B: Up-regulation of miR-146a increases the sensitivity of non-small cell lung cancer to DDP by downregulating cyclin J. BMC Cancer 17: 138, 2017.
50. Yuwen DL, Sheng BB, Liu J, Wenyu W and Shu YQ: miR-146a-5p level in serum exosomes predicts therapeutic effect of cisplatin in non-small cell lung cancer. Eur Rev Med Pharmacol Sci 21: 2650-2658, 2017.
51. Gan L, Sun T, Li B, Tian J, Zhang J, Chen X, Zhong J, Yang X and Li Q: Serum miR-146a and miR-150 as potential new biomarkers for hip Fracture-induced acute lung injury. Mediators Inflamm 2018: 8101359, 2018.
52. Freem LJ, Escot S, Tannahill D, Druckenbrod NR, Thapar N and Burns AJ: The intrinsic innervation of the lung is derived from neural crest cells as shown by optical projection tomography in Wnt1-Cre;YFP reporter mice. J Anat 217: 651-664, 2010.
53. Zhao Y, Haney MJ, Gupta R, Bohnsack JP, He Z, Kabanov AV and Batrakova EV: GDNF-transfected macrophages produce potent neuroprotective effects in Parkinson's disease mouse model. PLoS One 9: e106867, 2014.
54. Huang S, Yang L, An Y, Ma X, Zhang C, Xie G, Chen ZY, Xie J and Zhang H: Expression of hedgehog signaling molecules in lung cancer. Acta Histochem 113: 564-569, 2011.
55. Jiang Y, Han Y, Sun C, Han C, Han N, Zhi W and Qiao Q: Rab23 is overexpressed in human bladder cancer and promotes cancer cell proliferation and invasion. Tumour Biol 37: 8131-8138, 2016.